

Surface treatment of Ti and Ti composites using concentrating solar power and laser

Jaroslav Kováčik^{1*}, Štefan Emmer², José Rodríguez³, Inmaculada Cañadas³, Peter Šugár⁴, Jana Šugárová⁴, Barbora Bočáková⁴, Naďa Beronská¹

¹Institute of Materials & Machine Mechanics, Slovak Academy of Sciences, Slovakia

²IVMA STU, Slovakia

³Plataforma Solar de Almeria, Spain

⁴Slovak University of Technology in Bratislava, Faculty of Materials Science and Technology in Trnava, Institute of Production Technologies, Slovakia

Orcid: J. Kováčik (0000-0002-6970-0406), I. Cañadas (0000-0001-8637-1547), P. Šugár (0000-0002-9499-5672), J. Šugárová (0000-0002-3468-2148), B. Bočáková (0000-0002-4549-3908), N. Beronská (0000-0003-1527-922X)

Abstract: Titanium and its composites are widely used in implants of bones and teeth. Besides mechanical properties also surface characteristics are very important in these biomaterials. Very important are properties such as surface topography, roughness, chemistry, and surface energy, wettability, and Ti oxides or Ti nitride layers thickness. The concentrated solar power was used successfully to nitride Ti Grade 2 and powder metallurgical Ti prepared from hydrogenated dehydrogenated Ti powder. The nitriding experiments were performed under nitrogen atmosphere at different temperatures and time in SF40 (40kW horizontal solar furnace) at PSA, Spain. Concentrated solar energy has been shown to be an economical alternative to conventional gas nitriding techniques in electric furnaces, CVD, PVD, plasma nitriding, or laser treatments. It significantly shortens the heating time (heating rates 100 K/min), it creates a continuous δ -TiN and ϵ -Ti₂N nitride layer on all surfaces of the samples and optimum nitriding is 5 minutes at 900°C. It has been observed that the solar process represents a significant reduction of the heating time to several minutes (up to 5 minutes at temperature range 500-1000 °C), a clean and non-polluting high-temperature process. The formation of continuous and homogeneous surface layers of TiN, Ti₂N and their mixture according to the nitriding temperature was investigated using X-ray diffraction and electron microscopy. Laser surface treatment is of great significance in modifying surface morphology and surface and near-surface region microstructures. Effects of laser treatment parameters on machined surface morphology, surface roughness and chemistry are analysed in this study and discussed from the point of view of application in dental implantology. The current advances of our research group in application of laser-treated powder metallurgy prepared Ti-based materials are analysed and discussed.

Keywords: surface treatment, titanium, titanium composites, concentrated solar power, laser.

1. Introduction

Titanium (Ti) and titanium alloys are more and more being used in various applications from aviation to biomedicine due to their excellent strength, high melting point, low density, high strength-to-weight ratio, excellent corrosion resistance, high fracture toughness, good heat transfer properties and biocompatibility [1, 2]. As biomedical implants, they are used in orthopaedic and dental fields, as bone plating, hard tissue replacements and screws [3–6]. Some surface micro-morphology modification technologies are used to improve biocompatibility and enhance osseointegration of the titanium implants. Osseointegration - the structural linkage made at the contact point where the human bone and the surface of an implant meet is supported by the implant surface porosity, surface roughness or by regular surface pat-

terns (texture) with texture elements smaller than 100 mm [7,8]. These structures may be fabricated by different technologies, such as sintering, sandblasting [9], chemical etching [10], plasma spraying [11], electrical discharge machining [12], electron beam texturing etc., including laser beam micro-machining [13–16] and solar nitriding [17].

Titanium-based metal matrix composites represent a new generation of biomaterials with superior properties and cost-effective production methods compared to conventional metallurgical methods. A great effort to develop this kind of material through different manufacturing processes in order to optimize their structure, mechanical properties and surface treatment could be found in many studies [18-31]. In addition to all the research,

* Corresponding author.
Email: ummsjk@savba.sk



there are many questions regarding the optimal surface morphology that have not yet been answered. Ti powder metallurgy (PM) is a cost-effective method of direct production of complex 3D Ti parts [32]. Thanks to this the authors decided to study laser micromachining of Ti – graphite composite samples, prepared by pioneering modified warm compaction PM method. In this study, the effect of laser energy on the morphology, roughness and chemistry of the machined surface was investigated and evaluated and discussed in terms of application in dental implantology. Moreover, in this study, samples of Cp Ti Grade 2 and pure PM Ti samples were gas nitrified using concentrated solar energy under nitrogen gas flow.

2. Experimental

The modified warm compaction method for producing of Ti and Ti composites was developed by Balog et al. for the dental [20, 33, 34] and by Sugar et al. for biomedical applications [35-37]. The Ti powder/ Ti composites were pre-compacted by cold isostatic pressing (CIP) at 200 MPa. Then CIP blanks were put into the sleeves (containers made from Cu,Al) - wall thickness of 3 mm, diameter of 30 mm. Then they were instantly pressed by uniaxial vacuum hot pressing (VHP) at 500 MPa, vacuum of 8 Pa, at 470 °C. CIPs and also sleeves were fully consolidated by direct extrusion (DE) into rod bars with a diameter of 6 mm using a flat face die (reduction ratio 16:1, ram speed of 10 mm.s⁻¹). The extrusion temperature range was 450 - 500°C. Achieved theoretical density of HDH Ti powder were above 99%.

Bulk commercial CP Ti Grade 2 (CP Ti Gr2) material was used for gas nitriding in solar furnace (Bibus Metals AG, Germany). It was 1 mm thick sheet cut into 15 x 10 mm rectangles in as received state (no cleaning or polishing of sample surface takes place). Other material was PM prepared bulk compact made from (Fig. 1) HDH Ti powder (below 150 mm, purity 99.4 %, Kimet Special Metal Precision Casting Co., Ltd., Hengshui, China) using warm compaction [33]. PM pieces from used tensile test samples with M5 threads and machined inner holes were used for nitriding. The theoretical density of used PM Ti samples was 99.13 %, elastic modulus 94.5 GPa, yield stress $R_{p0.2}$ 541 MPa, ultimate tensile strength of 687 MPa and elongation to fracture of 4.08 %. O, N and H content is 0.207 wt.%, 0.010 wt.% and 0.026 wt. %, respectively.

SF5 vertical solar furnace [38] at Plataforma Solar de Almeria, Spain was used for solar nitriding experiments. SF5 solar furnace works in a vertical axis – optical axis of heliostat and parabolic concentrator is vertically aligned. The main advantage of this is that the focus area is arranged in a horizontal plane; therefore, the samples could be freely placed and no fixation is needed. The PM Ti sample was positioned on Mo plate (200 x 200 x 0.7 mm) and both of them on ZrO₂ plate (400 x 400 x 3 mm). Conversely, the CP Ti Gr 2 sheets were placed directly on ZrO₂. The samples were nitride in spherical vacuum chamber of a 5L Duran borosilicate sphere,

which is closed at the bottom by a cooled flange secured by an O-ring and a clamp. Pfeiffer turbomolecular pump is used to evacuate the chamber. The sample was positioned so that it was at the optimal focus distance. The size of the sunspot was approximately 50 mm. During experiments, the chamber primary evacuated (the vacuum of 0.8 Pa) and then nitrogen gas flow (400 l/h, pressure of 3 bar, technical purity) was used.

The thermocouple placed at bottom of Mo plate for PM

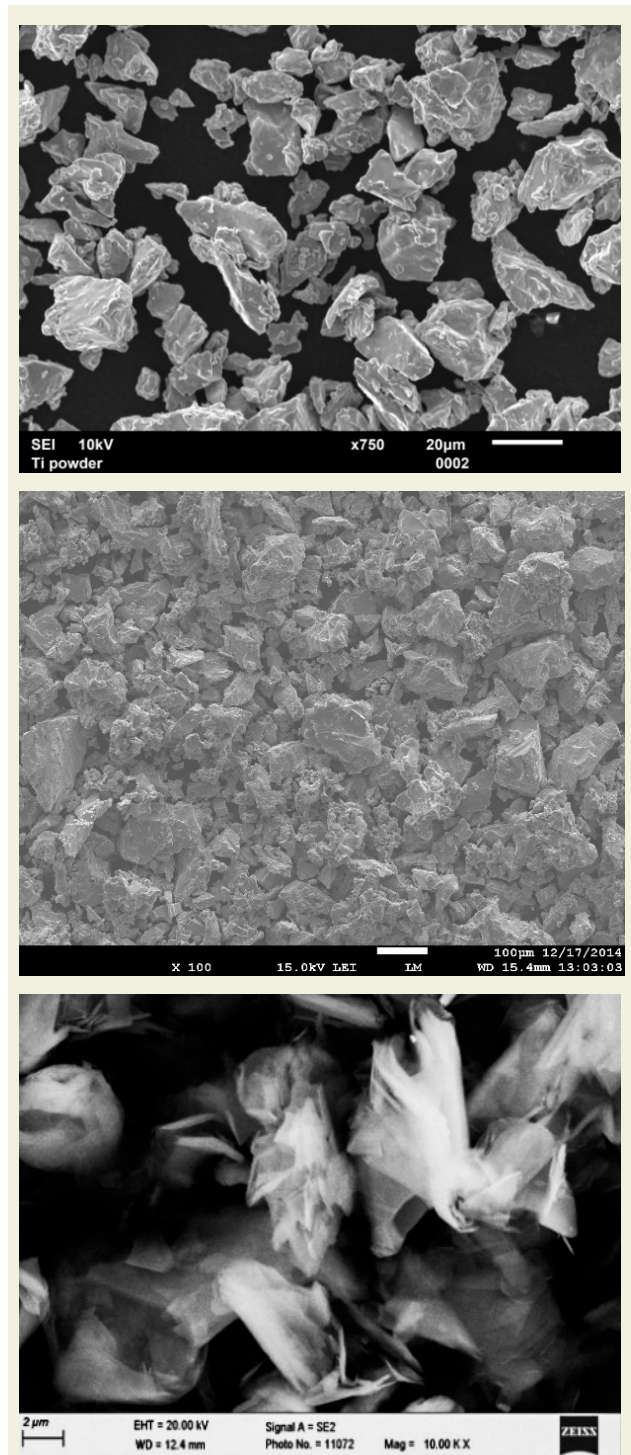


Figure 1. Characteristic shape of powders: HDH titanium powders: up left - Ti powder below 30 mm, up right - Ti powder below 150 mm, and bottom - graphite flakes below 16 mm. [36]

Ti samples and directly at bottom of CP Ti Gr 2 sheets was used to control the temperature. A constant heating/cooling rate of 100 K/min was used during the experiments. Complex PM samples were nitrided at 600 °C for 30 seconds, at 750 °C for 30 seconds and 5 min. A set of CP Ti Gr 2 sheets were nitrided for 1 and 5 min at 700, 800, 900 and 1000 °C, respectively.

Further, Ti MMC experimental samples were prepared from HDH titanium powder (particle size below 30 μm , Kimet Special Metal Precision Casting Co., Ltd., Hengshui, China) and 15.0 vol. % of graphite flakes (Fig. 1). Ti powder shows a typical fragmented angular shape. Graphite flakes (purity of 99.9%) have particle size of 16 μm with aspect ratio of 10. Powder mixture was CIPed at 200 MPa and then compacted by hot vacuum pressing at 450 °C under 500 MPa [36]. Density of the samples was determined by weighing and volume measurement in the range of 4.10–4.15 $\text{g}\cdot\text{cm}^{-3}$. Then the porosity was calculated using theoretical density 4.23 $\text{g}\cdot\text{cm}^{-3}$: 2.44% \pm 0.15%. Finally, the cylinders with a diameter of 24 mm and a height of 5 mm were cut. The cylinders were encapsulated using copper-based ProbeMet conductive mounting. Then, their surfaces were ground with 1200 grit sandpapers to be prepared for laser beam micromachining.

Lasertec 80 Shape (DMG MORI GmbH, München, Germany) machining equipment is based on 1064 nm wavelength nanosecond fibre Y-doped laser. Six 6 x 6 mm

square surfaces were ablated by combining different values of pulse energy (E_p), lateral pulse distance (D_L) and different lateral pulse overlaps (O_L) (Fig. 2). The result was different thermal energy density. Constant pulse duration 120 ns and 50 μm laser spot diameter (D) were used during all experiments. As shows Fig. 2 bi-directional traces layout – “cross-hatching strategy” was employed.

The motion strategy of the laser beam micromachining is following: Fig. 2a - scheme of pulses overlaps, D laser spots diameter, D_L lateral pulse distance, D_T transverse pulse distance, O_L lateral overlap and O_T is transverse overlap; Fig. 2b shows the scheme of two ablated layers creation in Ar gas flow rate of 10 l/min. The transverse pulse overlap (O_T) is of 80%.

After the experiments the samples were prepared for microstructure observations. Microstructure of samples was observed at PSA's Materials Lab using Leica DMI 5000 Minverted digital microscope and at IMMS SAS using scanning electron microscope JEOL 7600F, equipped with a Schottky thermal-emission cathode (thermal FEG - W-coated ZrO₂) as well as energy and wavelength spectrometers from Oxford Instruments. X-ray diffraction (XRD) patterns were measurement using a Bruker D8 diffractometer (Bruker, Billerica, MA, US) - Cu-K α X-rays of wavelength $\lambda = 1.5406 \text{ \AA}$ was used to verify phases transformations for the 2θ range 15° - 105° and step 0.05°.

3. Results and Discussion

3.1. Gas nitriding in Solar furnace

The results confirmed that the concentrated solar power can be employed for nitriding of titanium thus diminishing CO₂ footprint and overall energy consumption. The nitride layer created in solar furnace was continuous and covers all surfaces of complex 3D product. PM Ti samples threads and holes were nitrided successfully (Fig. 3).

During creation of the nitride layers, beneath of them solid solution of $\alpha\text{-Ti(N)}$ is continually created and growth due the diffusion of nitrogen into titanium base material. Therefore, it was necessary to estimate optimal time and temperature for the nitridation at solar furnace and it was done on CP Ti Gr2 samples (Fig. 4). It was observed that with increasing temperature and/or time of gas nitriding the thickness of nitride layer increases. For example, for CP Ti Gr 2 samples gas nitrided in solar furnace for 1 minute at 900°C and 1000°C the 15 mm thick nitride layers increased up to 50 μm , respectively. Anyway, pores could be observed prepared layers. This could be caused by volumetric changes during phase transformations between $\delta\text{-TiN}$ and $\epsilon\text{-Ti}_2\text{N}$ nitrides inside the layer.

In general, nitride formation involves the adsorption of nitrogen on the metal surface. Furthermore, the nitrogen concentration profiles in the metal will be controlled by diffusion laws and temperature. The diffusion occurs in a polycrystalline Ti substrate mostly along grain bound-

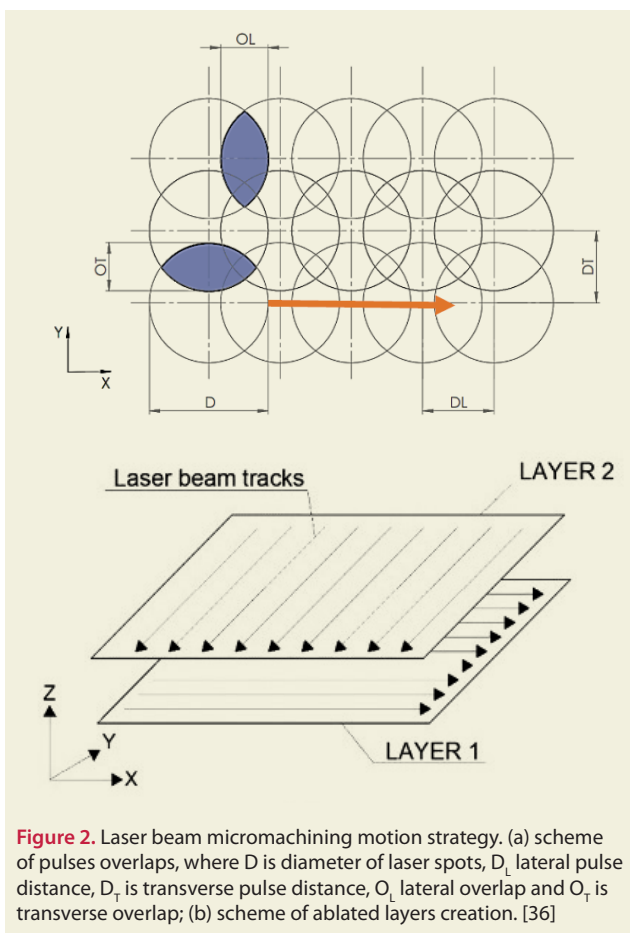


Figure 2. Laser beam micromachining motion strategy. (a) scheme of pulses overlaps, where D is diameter of laser spots, D_L lateral pulse distance, D_T is transverse pulse distance, O_L lateral overlap and O_T is transverse overlap; (b) scheme of ablated layers creation. [36]

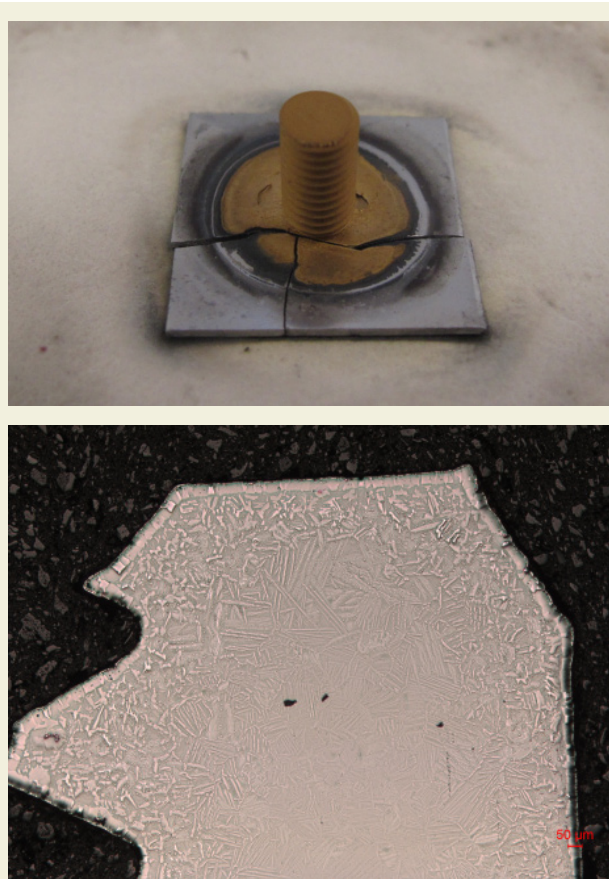


Figure 3. PM Ti nitrided sample coloured in yellow after using of concentrated solar power -left, and PM Ti sample microstructure after nitridation at 750 °C for 5 minutes: thread and the hole (light microscopy) - right

aries. This lowers the activation barrier and increases nitrogen diffusion coefficient. The formation of nitrides first occurs on the surface of the substrate, because in this position the minimum nitrogen content of 33% is simply reached. After that, the hexagonal crystal lattice of titanium changes towards the FCC lattice of titanium nitride (NaCl-type crystal) [39].

Nitrided layer is composed of Ti_2N and TiN, followed by diffusion zone - an interstitial solution of nitrogen in α or β titanium phases depending on temperature and composition. X-ray analysis showed that on the surface of the investigated Ti samples both δ - TiN and ε - Ti_2N are present. As X-ray penetration depth is relatively small for bulk materials, α -Ti peaks were not observed. It can be concluded, that the thickness of nitrides layer is over 20 mm (see Fig. 5).

3.2. Laser surface treatment

In Figure 6 SEM micrographs are presented of the laser machined surfaces for different energies at various magnifications. During the experiments the main role plays energy of laser pulse - E_T is total energy input to the material per illuminated area calculated for one layer. Usually it is energy of laser impulse times number of pulses per layer [36]. After laser treatment, on all surfaces the melted and then rapidly solidified layer of Ti MMC



Figure 4. CP Ti Gr2 sheets before (grey) and after (yellow) gas nitriding at SF5 solar furnace – left. CP Ti Gr2 sample microstructure (SEM) after nitriding in solar furnace (1 minute, 1000°C) and corresponding thickness of TiN layer - right.

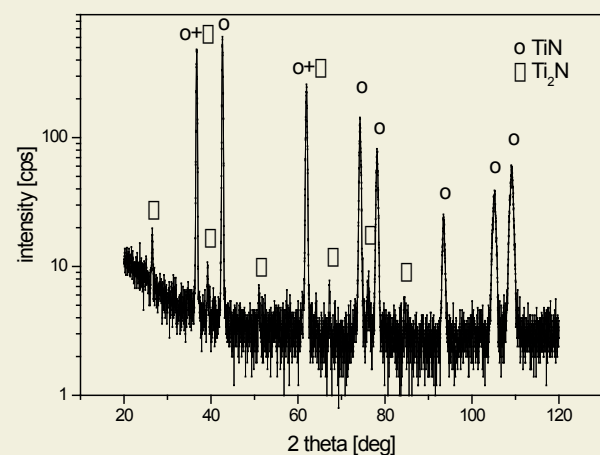


Figure 5. CP Ti Gr2 sample X-ray analysis after nitridation in solar furnace (1 minute, 900 °C).

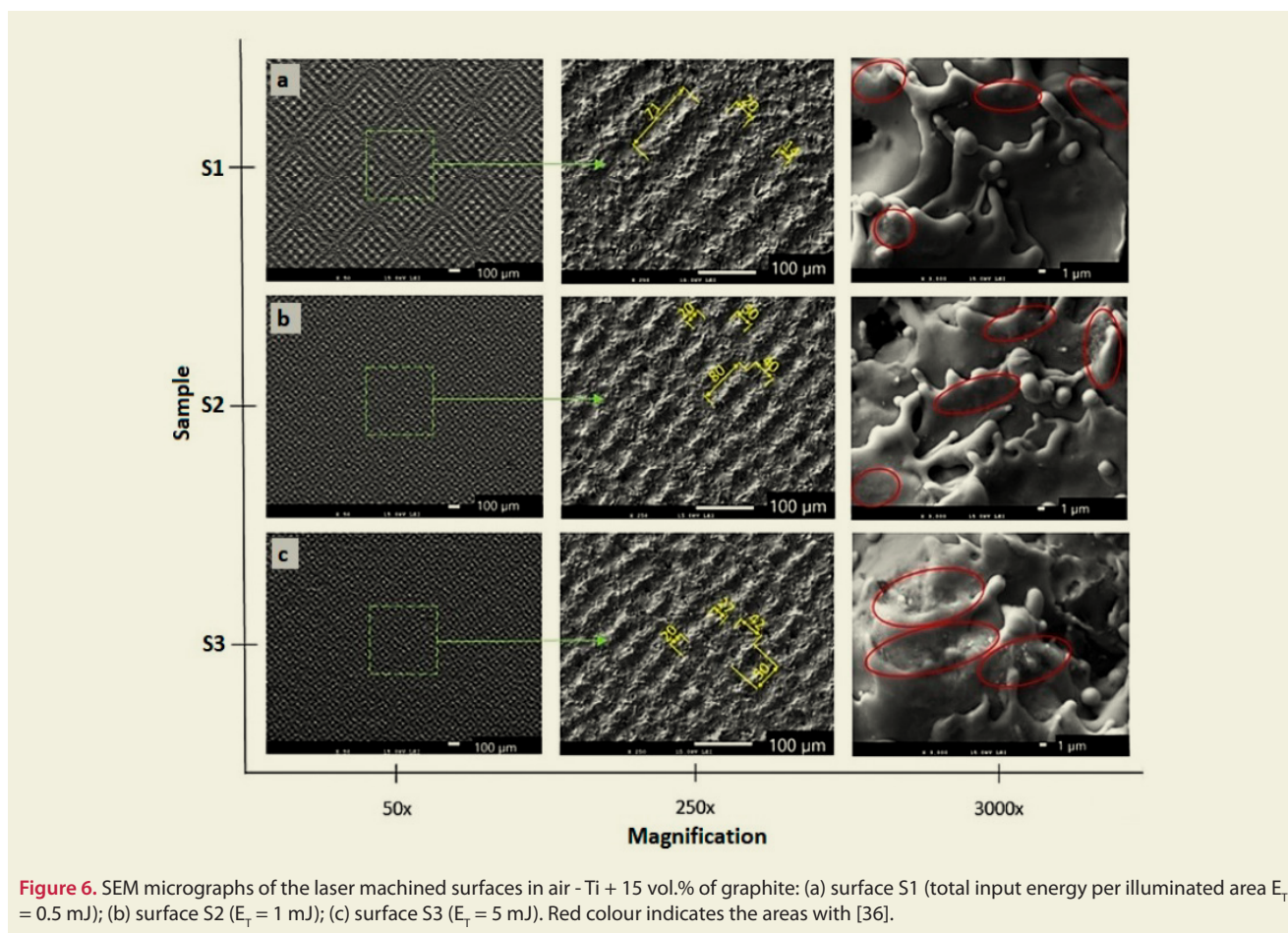


Figure 6. SEM micrographs of the laser machined surfaces in air - Ti + 15 vol.% of graphite: (a) surface S1 (total input energy per illuminated area $E_T = 0.5$ mJ); (b) surface S2 ($E_T = 1$ mJ); (c) surface S3 ($E_T = 5$ mJ). Red colour indicates the areas with [36].

(15 vol.% graphite) material is visible. Depending on the input energies three different types of surfaces were observed. The first structure type is formed by visible laser beam paths forming square texture thanks to the used cross-hatching strategy (Figure 6a). The second surface type is formed by the protrusions forming a square-shaped texture, but of small size (Figure 4b,c). EDS analysis of the laser machined indicated the presence of Ti, C and oxygen in all analysed surfaces. Non-irradiated

(N) surface possesses smallest concentration of oxygen. The oxygen concentration of laser machined surfaces increased with increasing value of input radiation energy. It was changed from 5.5 wt.% oxygen for N surface to 23.2 wt.% for maximal energy pulse. The RTG diffraction results of the laser machined surfaces showed the presence of the titanium, titanium monoxide and Ti_2O_3 peaks.

During machining in air (Fig. 6) a structure with more pronounced (sharper) edges and protrusions was formed on the surface. When machining in argon, the rounded edges of the solidified melt and droplets of spherical material with the presence of cracks on the sample were clearly visible (Fig. 7). The reason could be a different mechanism of solidification of the material during machining in air and during the action of argon at the machining site.

Samples (Fig. 7) showed the presence of pores with an approximate size of 1 μ m. Exceptionally, there were pores with cracks around the perimeter. The cracks could have been initiated by a high rate of heating and subsequent cooling, creating a high temperature gradient. On air-machined surfaces, pores were observed only in exceptional cases, which may be due to the presence of oxide layers. Another cause could be faster cooling and stresses in the material due to the flow of argon to the machining site. From the implants point of view, these cracks do not have a negative impact on the biocompatible properties of the

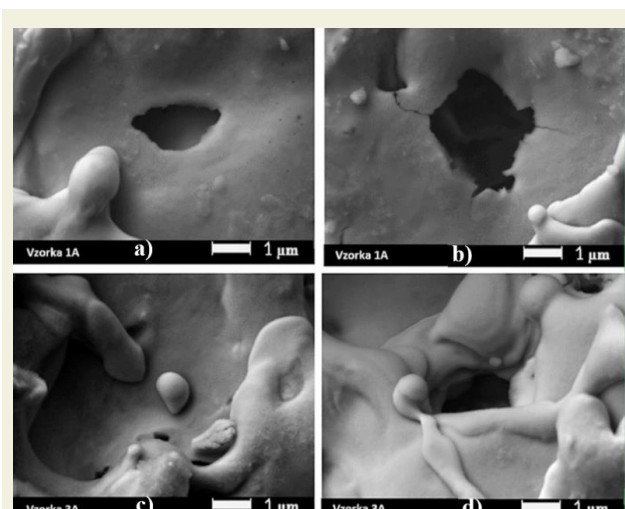


Figure 7. SEM images of the surfaces of the Ti MMC (15 vol.% graphite) samples laser processed in argon a) pore, $E_T = 0.5$ mJ; b) pore with cracks, $E_T = 0.5$ mJ; c) re-melted cavity, $E_T = 5$ mJ; d) pore with re-melted raised edges $E_T = 5$ mJ.

surface. Pores with these dimensions are suitable from the point of view of biocompatibility of the material and it is assumed that they do not affect the mechanical properties.

4. Conclusion

It was confirmed that concentrated solar power could be free energy alternative to conventional techniques of titanium nitriding.

SF5 - 5kW vertical solar furnace at Plataforma Solar de Almeria, Tabernas, Spain was used for nitriding of PM titanium and CP Ti Gr2 at different temperatures. The solar nitriding has following advantages when compared to conventional methods: It is non-polluting high-temperature clean method. It significantly shortens the heating time due to high heating rates up to 100 K/min. It allows to create a continuous δ -TiN and ϵ -Ti₂N nitride layer on all surfaces of the samples. Optimum nitriding times appear to be 5 minutes at 900°C.

Laser surface machining of Ti MMC composite with 15 vol.% of graphite in air and Ar atmosphere were performed with various laser pulse energy using cross-hatching strategy. The following conclusions can be drawn:

With a suitable combination of input parameters of the laser micromachining process, it is possible to achieve a regular texture on the composite material. The laser-treated surface consists of raised ridges of molten sol-

id spheres, cavities and craters. Documented deep valleys and ridges were associated with higher ablation energy intensity. As the pulse distance increased, the amount of oxygen on the surface decreased slightly according to EDS. Only of two types of titanium oxides - TiO and Ti₂O₃ - were confirmed on all surfaces using RTG analysis. Titanium dioxide has not been observed at all. A lower total energy level (lower pulse energy plus longer lateral pulse distances) is recommended to achieve favourable antibacterial surface properties. Higher total energies (higher pulse energies + shorter pulse distances) seems to be suitable for surfaces that can improve bone healing.

For more broad application of the investigated material, it is necessary to carry out another series of experiments, mainly aimed at an accurate description of the relationship between the structure of surface and the phenomenon of osseointegration.

5. Acknowledgements

The research was performed under Slovak national projects VEGA 2/0135/20 and VEGA 2/0054/23. Financial support by the Access to Research Infrastructures activity in the 7th Framework Programme of the EU (SFERA Grant Agreement n. 228296 and SFERA 2 Grant Agreement n. 312643) is gratefully acknowledged. We thank the Plataforma Solar de Almeria (PSA), Spain for providing access to its installations, the support of its scientific and technical staff, and the financial support of the SFERA-III project (Grant Agreement No 823802).

References

- [1] Cui Ch., Hu B., Zhao L., and Liu S., (2011) "Titanium alloy production technology, market prospects and industry development", *Materials & Design*, 32(3), pp.1684-1691
- [2] Selvan J. S., Subramania, K., Nath A.K. et al., (1998) "Hardness, microstructure and surface characterization of laser gas nitrided commercially pure titanium using high power CO₂ laser", *J. of Mater. Eng and Perform*, 7(5), pp. 647-655.
- [3] Banerjee D. and Williams J.C., (2013) "Perspectives on titanium science and technology", *Acta Mater.* 61, pp. 844–879.
- [4] Babuska, V., Palan J., Kolaja D., Kulda V., Duchek M., Cerny J. and Hrusak D. (2018) "Proliferation of Osteoblasts on Laser-Modified Nanostructured Titanium Surfaces", *Materials* 11, 1827.
- [5] Ozcan M. and Hammerle C., (2012) "Titanium as a reconstruction and implant material in dentistry: Advantages and pitfalls.", *Materials* 5, pp. 1528–1545.
- [6] Cordeiro M.J. and Barão, R.A.V., (2017) "Is there scientific evidence favoring the substitution of commercially pure titanium with titanium alloys for the manufacture of dental implants?", *Mater. Sci. Eng. C*, 71, pp. 1201–1215.
- [7] Rupp F., Liang L., Geis-Gerstorf J., Scheideler L. and Hüttig F., (2018) "Surface characteristics of dental implants: A review.", *Dent. Mater.*, 34, pp.40–57.
- [8] Kurella A. and Dahotre N., (2005) "Review paper: Surface Modification for Bioimplants: The Role of Laser Surface.", *J. Biomed. Appl.*, 20, pp. 5–50.
- [9] Lin Y., Huang C.F., Cheng H.C. and Shen, Y.K. (2013) "A modified surface on titanium alloy by micro-blasting process.", *Adv. Mater. Res.*, 797, pp. 696–699.
- [10] Nazarov D.V., Zemtsova E.G., Solokhin A., Valie, R.Z. and Smirnov, V.M. (2017) "Modification of the surface topography and composition of ultrafine and coarse grained titanium by chemical etching.", *Nanomaterials*, 7, 15.
- [11] Chappuis V., Buser R., Bragger U., Bornstein M.M., Salvi G.E. and Buser D., (2013) "Long-term outcomes of dental implants with a titanium plasma-sprayed surface: A 20-year prospective case series study in partially edentulous patients." *Clin. Implant Dent. Relat. Res.*, 15, pp. 780–790.
- [12] Lee W.F., Yang T.S., Wu Y.C. and Peng P.W., (2013) "Nanoporous biocompatible layer on Ti–6Al–4V alloys enhanced osteoblast-like cell response." *J. Exp. Clin. Med.*, 5, pp. 92–96.
- [13] Mura D.M., Dini G., Lanzetta M. and Rossi, A., (2018) "An experimental analysis of laser machining for dental implants." *Procedia CIRP*, 67, pp. 356–361.
- [14] Braga F.J.C., Marques R.F., de A Filho E. and Guastaldi, A.C., (2007) "Surface modification of Ti dental implants by Nd:YVO₄ laser irradiation.", *Appl. Surf. Sci.*, 253, pp. 9203–9208.
- [15] Xue W., Krishna V.B., Bandyopadhyay A. and Bose, S., (2007) "Processing and biocompatibility evaluation of laser processed porous titanium", *Acta Biomater.*, 3, pp. 1007–1018.
- [16] Ciganovic J., Stasic J., Gakovic B., Momcilovic M., Milovanovic D., Bokorov M. and Trtica M., (2012) "Surface modification of the titanium implant using TEA CO₂ laser pulses in controllab-

- le gas atmospheres—Comparative study.” *Appl. Surf. Sci.*, 258, pp. 2741–2748.
- [17] Rodriguez G.P, Herranz G. and Romero A., (2013) “Solar gas nitriding of Ti6Al4V alloy”, *Applied Surface Science*, Vol. 283, pp. 445–452
- [18] Jiang S., Huang L.J., An Q., Geng L., Wang X.J. and Wang S., (2018) “Study on titanium-magnesium composites with bicontinuous structure fabricated by powder metallurgy and ultrasonic infiltration.”, *J. Mech. Behav. Biomed. Mater.*, 81, pp. 10–15.
- [19] Balog M., Snajdar M., Krizik P., Schauerl Y., Stanec Y. and Catic A., “Titanium-Magnesium Composite for Dental Implants (BIACOM).” In *TMS 2017 146th Annual Meeting & Exhibition Supplemental Proceedings The Minerals, Metals & Materials Series* Springer: Cham, Switzerland, 2017 p. 271–284.
- [20] Balog M., Ibrahim H.M.A., Krizik P., Bajanaa O., Klimova A., Catic A. and Schauerl Z., (2019) “Bioactive Ti + Mg composites fabricated by powder metallurgy: The relation between the microstructure and mechanical properties.” *J. Mech. Behav. Biomed. Mater.*, 90, pp. 45–53.
- [21] Bandyopadhyay A., Dittrick S., Gualtieri T., Wu J. and Bose, S., (2016) “Calcium phosphate–titanium composites for articulating surfaces of load-bearing implants.”, *J. Mech. Behav. Biomed. Mater.*, 57, pp. 280–288.
- [22] Gemelli E., Jesus J., Camargo N.H.A., Soares G.A., Henriques V.A.R. and Nery F., (2012) “Microstructural study of a titanium-based biocomposite produced by the powder metallurgy process with TiH₂ and nanometric -TCP powders.”, *Mater. Sci. Eng. C*, 32, pp.1011–1015.
- [23] Karanjai M., Sundaresan R., Rao G.V.N. and Tallapragada, R.M.R., (2007) “Development of titanium based biocomposite by powder metallurgy processing with in situ forming of Ca–P phases.” *Mater. Sci. Eng. A*, 447, pp.19–26.
- [24] Han C., Wang Q., Song B., Li W., Wei Q., Wen S., Liu J. and Shi Y., (2017) “Microstructure and property evolutions of titanium/nano-hydroxyapatite composites in-situ prepared by selective laser melting.” *J. Mech. Behav. Biomed. Mater.*, 71, pp. 85–94.
- [25] Miranda G., Araújo A., Bartolomeu F., Buciumeanu M., Carvalho O., Souya J.C.M., Silva F.S. and Henriques B., (2019) “Design of Ti6Al4V-HA composites produced by hot pressing for biomedical applications.”, *Mater. Des.*, 108, pp. 488–493.
- [26] Alshammari Y., Yang F. and Bolzoni L., (2019) “Mechanical properties and microstructure of Ti-Mn alloys produced via powder metallurgy for biomedical applications.”, *J. Mech. Behav. Biomed. Mater.*, 91, pp.391–397.
- [27] Gain K.A., Zhang L. and Quadir Z.M., (2016) “Composites matching the properties of human cortical bones: The design of porous titanium-zirconia (Ti-ZrO₂) nanocomposites using polymethyl methacrylate powders.” *Mater. Sci. Eng. A*, 662, pp. 258–267.
- [28] Li Y., Munir S.K., Lin J. and Wen C., (2016) “Titanium-niobium pentoxide composites for biomedical applications” *Bioact. Mater.*, 1, pp. 127–131.
- [29] Shahali H., Jaggessar A. and Yarlagadda P.K., (2017) “Recent advances in manufacturing and surface modification of titanium orthopaedic applications.” *Procedia Eng.*, 174, pp.1067–1076.
- [30] Asri R.I.M., Harun W.S.W., Samykano M., Lah N.A.C., Ghani S.A.C., Tarlochan F. and Raza M.R., (2017) “Corrosion and surface modification on biocompatible metals: A review.” *Mater. Sci. Eng. A*, 77, pp. 1261–1274.
- [31] Alla K.R., Ginjupalli K., Upadhy N., Shammam M., Ravi R.K. and Sekhar R., (2011) “Surface roughness of implants: A review.” *Trends Biomater. Artif. Organs*, 25, pp.112–118.
- [32] Ma, Q., Francis, H. and Sam, F. (2015) *Titanium Powder Metallurgy*, Butterworth-Heinemann: Boston, MA, USA
- [33] Balog M., Viskic J., Krizik P., Schauerl Z., Snajdar M., Stanec Z. and Catic, A., (2016) “CP Ti fabricated by low temperature extrusion of HDH powder: Application in dentistry.” *Key Eng. Mater.*, 704, pp. 351–359.
- [34] Ibrahim A.M.H., Takacova M., Jelenska L., Csaderova L., Balog M., Kopacek J., Eliska S. and Krizik P., (2021) “The effect of surface modification of TiMg composite on the in-vitro degradation response, cell survival, adhesion, and proliferation”, *Materials Science and Engineering: C*, Vol. 127, , 112259.
- [35] Šugár P., Kováčik J., Šugárová J. and Ludrovová B., (2019) “A Study of Laser Micromachining of PM Processed Ti Compact for Dental Implants Applications.” *Materials*, 12, 2246.
- [36] Šugár P., Ludrovová B., Kováčik J., Sahul M. and Šugárová, J., (2020) “Laser-Based Ablation of Titanium–Graphite Composite for Dental Application.” *Materials*, 13, 2312.
- [37] Šugár P., Ludrovová B., Kalbáčová M.H., Šugárová J., Sahul M. and Kováčik J., (2021) “Laser Surface Modification of Powder Metallurgy-Processed Ti-Graphite Composite Which Can Enhance Cells’ Osteo-Differentiation.” *Materials*, 14, 6067.
- [38] Rodríguez J., Cañadas I. and Zarza E., (2013), PSA vertical axis solar furnace SF5, *Energy Procedia*, 49, p. 1511–1522
- [39] Scardi P., Tesi B., Bacci T. and Gianoglio C., (1990) “Characterization Of Ion-Nitrided Titanium Layers By Means Of X-Ray Microdiffractometry”, *Surface and Coatings Technology*, Vol. 41, pp. 83 – 91